# NUMERICAL STUDY OF IMPERFECT LIQUID-FILLED CONICAL SHELLS

## Verifying the Present Design Rule

Wesley Vanlaere [a], Guy Lagae [a], Werner Guggenberger [b], Rudy Van Impe [a]

[a] Ghent University, Laboratory for Research on Structural Models, Ghent, Belgium
[b] Graz University of Technology, Institute for Steel Structures and Shell Structures, Graz, Austria

## INTRODUCTION

Liquid-filled conical shells can typically be found in a steel water tower where the conical vessel acts as a water reservoir. The presence of the liquid in the thin-walled steel shell leads to compressive stresses in meridional direction and tensile stresses in circumferential direction. This meridional compressive stress increases rapidly along the generators of the cone between the liquid surface and the base of the cone. If this compressive stress surpasses a certain critical level, the shell buckles despite the stabilising effect of the tensile hoop stresses. This elastic buckling phenomenon entails the failure of the entire structure. The combination of the meridional compressive stress and the hoop stress can also lead to a second type of failure, i.e. yielding of the shell wall and thus plastic failure. For this failure phenomenon both stress components act together.

In the past, a number of water towers have collapsed due to these failure phenomena. This was the incentive for performing an elaborated series of experiments on liquid-filled conical shells by Vandepitte *et al.* [1,2]. On the basis of these experiments – most of which led to elastic buckling – a design rule was derived. This design rule is included in the 4th Edition of the ECCS Recommendations of Buckling of Shells [3] and will also be included in the 5th Edition of these Recommendations in a different format [4,5].

Although this rule has a solid experimental basis and has been successfully applied for more than two decades, it has never been the subject of a thorough and extensive numerical verification. This verification is however desirable for a number of reasons. Since we are dealing with thin-walled steel shell structures, imperfections tend to have an important effect on the failure stress. This effect is included in the design rule, but imperfections that appear in laboratory models are not necessarily representative for the imperfections of real structures. A second argument for this verification is the fact that the rule takes plasticity into account, although the number of experiments that led to (elastic-)plastic buckling was limited. Finally, the rule was given a new format for the forthcoming 5th Edition and has been slightly changed so that it can be applied in combination with the Eurocode quality classes and the capacity curve format for shell structures [6].

The goal of our present study is to do the numerical verification of the design rule in the format of the forthcoming 5th Edition. In this contribution, as a first step towards the verification, the results of the numerical simulations of seven cone geometries are compared with the design rule.

## 1 THE DESIGN RULE

In the forthcoming Fifth Edition of the ECCS Recommendations, the design rule for the liquid-filled conical shells leads to a stress design. The design meridional buckling stress is given as:

$$\sigma_{xRd} = \frac{\sigma_{xRk}}{\gamma_m} \text{ with } \gamma_m = 1{,}1. \quad (1)$$

In this equation, the characteristic meridional buckling stress $\sigma_{xRk}$ is determined as:

$$\sigma_{xRk} = \chi \cdot \sigma_{xRpl} \text{ with } \sigma_{xRpl} = \frac{f_{yk}}{\sqrt{1 + \frac{1}{\psi} + \left(\frac{1}{\psi}\right)^2}} \tag{2}$$

where $\psi$ is the ratio of the meridional stress and the absolute value of the hoop stress and $f_{yk}$ is the characteristic yield stress. The meridional stress at the lower rim of the shell is given by:

$$\sigma_x = \frac{\gamma' \cdot h'^2 \cdot \left(r_1 + \frac{h'}{3} \cdot \tan\beta\right) \cdot \tan\beta}{2 \cdot r_1 \cdot t \cdot \cos\beta}. \tag{3}$$

In this equation, the parameters are the specific weight $\gamma'$ of the liquid, the liquid height h', the radius of the lower rim $r_1$, the thickness of the shell t and the apex half angle of the cone $\beta$. The cone geometry is also given in *Fig. 1*. The circumferential tensile stress at the lower rim is given by:

$$\sigma_\theta = -\frac{\gamma' \cdot h' \cdot r_1}{t \cdot \cos\beta}. \tag{4}$$

The relative slenderness ratio of the cone is defined as:

$$\bar{\lambda} = \sqrt{\frac{\sigma_{xRpl}}{\sigma_{xRcr}}}. \tag{5}$$

The elastic critical buckling stress of the uniformly axially compressed conical shell is given by:

$$\sigma_{xRcr} = 0,605 \cdot E \cdot t \cdot \frac{\cos\beta}{r_1}. \tag{6}$$

The buckling strength reduction factor $\chi$ can be derived from the capacity curve which is given by the following equations:

$$\chi = 1 \qquad \text{when } \bar{\lambda} \le \bar{\lambda}_0 \tag{7}$$

$$\chi = 1 - \beta' \cdot \left(\frac{\bar{\lambda} - \bar{\lambda}_0}{\bar{\lambda}_p - \bar{\lambda}_0}\right)^\eta \qquad \text{when } \bar{\lambda}_0 \le \bar{\lambda} \le \bar{\lambda}_p \tag{8}$$

$$\chi = \frac{\alpha_{xpe}}{\bar{\lambda}^2} \qquad \text{when } \bar{\lambda}_p \le \bar{\lambda} \tag{9}$$

*Eq. (7)* describes the behaviour when failure occurs due to plastic buckling, *Eq. (8)* deals with elastic-plastic buckling and *Eq. (9)* describes elastic buckling. The $\beta'$, $\eta$ and $\bar{\lambda}_0$ are the plastic buckling parameters. The experiments that were performed by Vandepitte *et al.* [1,2] in the past didn't lead to enough data to derive values for these parameters. Therefore, the values for the axially compressed unstiffened cylinder were adopted, i.e. $\beta' = 0,6$; $\eta = 1$; $\bar{\lambda}_0 = 0,2$. This is recommended in the Eurocode [6] and should lead to a conservative design.

The value of the plastic limit relative slenderness $\bar{\lambda}_p$ is determined as:

$$\bar{\lambda}_p = \sqrt{\frac{\alpha_{xpe}}{1 - \beta'}}. \tag{10}$$

Based on the experimental results, the elastic imperfection reduction factor $\alpha_{xpe}$ is defined as:

$$\alpha_{xpe} = 0,50 \cdot \left(1 - \frac{1,50}{Q}\right) \cdot \left(\frac{r_1}{h'} \cdot \bar{p}\right)^{0,135 \cdot \left(1 + {}^{1,00}/_{Q}\right)}. \tag{11}$$

In this equation, $\bar{p}$ is the internal pressure parameter:

$$\bar{p} = \frac{|\sigma_\theta|}{\sigma_{xRcr}}. \tag{12}$$

The quality parameter Q is defined in the Eurocode [6]. The values are given in *Table 1*.

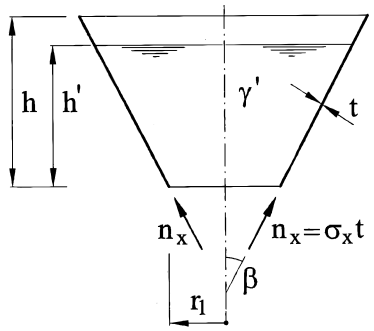


*Fig. 1.* The cone geometry

*Fig. 2.* Shape of the first eigenmode

*Table 1.* Values of the fabrication quality parameter Q [-]

| Quality | Description | Q |
|---|---|---|
| Class A | Excellent | 40 |
| Class B | High | 25 |
| Class C | Normal | 16 |

## 2 THE NUMERICAL SIMULATIONS

### 2.1 The Seven Cone Geometries

A first step towards the numerical verification of the design rule is made here by verifying the rule for seven cone geometries. In this investigation quality class C is assumed. The geometries are given in *Table 2*. The cones are filled with water up to a level where a slight increase would lead to failure according to the ECCS design rule. For each geometry, the design procedure – as described in Section 1 – is followed and the main results are also given in *Table 2*. The table shows that the procedure predicts elastic buckling except for cone geometry 2 and 7 where elastic-plastic buckling – and thus some influence of yielding – is to be expected.

For these seven geometries, numerical simulations with the finite element package ABAQUS were performed. In the simulations, the water level that causes instability $h'_{Rk}$ was determined. In the numerical model, the lower rim is simply supported (boundary condition BC1f) and the upper rim is free to deform (BC3). The simulations are geometrically and materially nonlinear and include geometrical imperfections (GMNIA). The material exhibits an elastic-perfect plastic behaviour. The imperfections are according to quality class C and have the maximal amplitude that is allowed for this quality class [6]. As imperfection shape, the first eigenmode of the perfect cone is taken. This is an axisymmetric mode with a number of waves in meridional direction. The imperfection shape is shown in *Fig. 2*. The radial deviations from the perfect shape along a meridian are plotted in *Fig. 3*. A positive value indicates an outward deviation, a negative value an inward deviation. For every GMNIA analysis, the sign of the imperfection amplitude was chosen such that the first half wave of the imperfection was oriented outward. This led to the lowest critical water levels $h'_{Rk}$. The results of the simulations are given in *Table 2* below the predictions of the design procedure.

*Table 2.* Comparison of the numerical results for the seven geometries with the design rule

| Number | 1 | 2 | 3 | 4 | 5 | 6 | 7 |
|---|---|---|---|---|---|---|---|
| $r_1$ (mm) | 90 | 3.000 | 350 | 579 | 200 | 3.794 | 3.794 |
| t (mm) | 0,3239 | 10 | 0,30 | 0,310 | 0,1229 | 8 | 15 |
| $\beta$ (°) | 49,93 | 45 | 40 | 40 | 39,98 | 51 | 51 |
| E ($N/mm^2$) | 195.420 | 210.000 | 210.000 | 200.000 | 5220 | 196.200 | 196.200 |
| $f_{yk}$ ($N/mm^2$) | 240 | 240 | 240 | 240 | elastic | 240 | 240 |
| ECCS stress design procedure | | | | | | | |
| $h'_{Rk}$ (mm) | 664 | 8050 | 907 | 872 | 124 | 5404 | 8389 |
| $\overline{\lambda}/\overline{\lambda}_p$ (-) | 1,39 | 0,95 | 1,67 | 1,67 | - | 1,07 | 0,94 |
| $\sigma_{xRk}$ (MPa) | 48,3 | 85,2 | 25,4 | 18,7 | 0,781 | 55,7 | 86,2 |
| ABAQUS GMNIA | | | | | | | |
| $h'_{Rk}$ (mm) | 737 | 6705 | 920 | 871 | 131 | 4442 | 6903 |
| $\sigma_{xRk}$ (MPa) | 64,5 | 54,4 | 26,3 | 18,7 | 0,887 | 35,2 | 53,5 |
| $\sigma_{xRk\ GMNIA}/\sigma_{xRk\ ECCS}$ (-) | 1,33 | 0,64 | 1,04 | 1,00 | 1,13 | 0,63 | 0,62 |
| ABAQUS GNIA | | | | | | | |
| $h'_{Rk}$ (mm) | 757 | 9318 | 916 | 900 | 131 | 6079 | 9705 |
| $\sigma_{xRk}$ (MPa) | 69,4 | 122,6 | 26,0 | 20,1 | 0,887 | 73,8 | 124,1 |
| $\sigma_{xRk\ GNIA}/\sigma_{xRk\ ECCS}$ (-) | 1,44 | 1,44 | 1,02 | 1,08 | 1,13 | 1,32 | 1,44 |

The ratios of the characteristic meridional buckling stresses $\sigma_{xRk\ GMNIA}/\sigma_{xRk\ ECCS}$ allow to determine whether the design rule leads to conservative results for these geometries. Apparently for geometries 2, 6 and 7 the design rule leads to unsafe results. The overprediction of the failure stress is almost 40%! Note that the $\overline{\lambda}/\overline{\lambda}_p$ -values for the problematic geometries are close to unity which indicates that yielding might have an influence. Investigations have confirmed this and showed that these unexpected low failure stresses are caused by early yielding. Due to the presence of an axisymmetric imperfection in the shape of the first eigenmode with the first half wave oriented outward, the stresses – mainly the circumferential but also the meridional – are much higher than the theoretical membrane stresses that are predicted by *Eqs. (3)* and *(4)*. This leads to locally elevated von Mises stresses, entailing early yielding and a plastic buckling phenomenon. This conclusion is confirmed by *Fig. 4* where the ratios of the stresses from the ABAQUS GMNIA analysis – at the mid surface – and the theoretical membrane stresses are plotted along the meridian for cone 2 at the load maximum. For the circumferential stress, this ratio has a peak up to almost 7! A similar conclusion was obtained with an approximate analytical method by Lagae *et al.* [7]. Finally, for the seven geometries, the numerical simulations were performed with elastic material behaviour (GNIA). The results of these simulations are also summarised in *Table 2* and indicate that without yielding the design rule leads to conservative results for all geometries. Note that compared to the GMNIA analyses the margin of safety increases for almost all the cones, even if the $\overline{\lambda}/\overline{\lambda}_p$ -values are well above 1.

### 2.2 Different Imperfection Shapes

In the previous section, it was shown that with an axisymmetric imperfection shape and an amplitude according to quality class C, the design rule may lead to unconservative results. In this

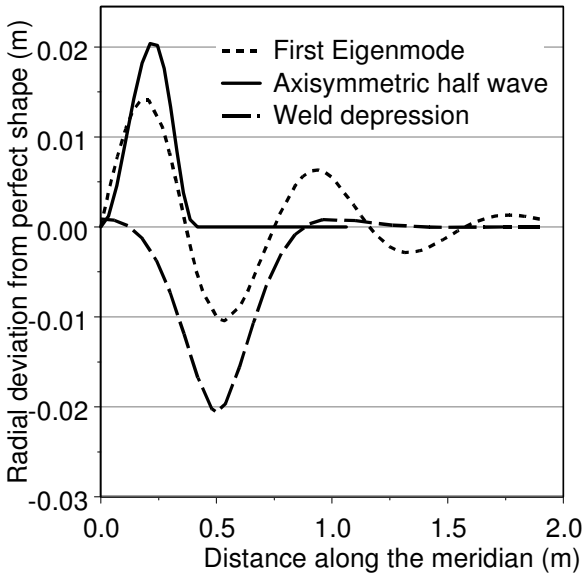


*Fig. 3.* The shape of the imperfections along the meridian of cone 2

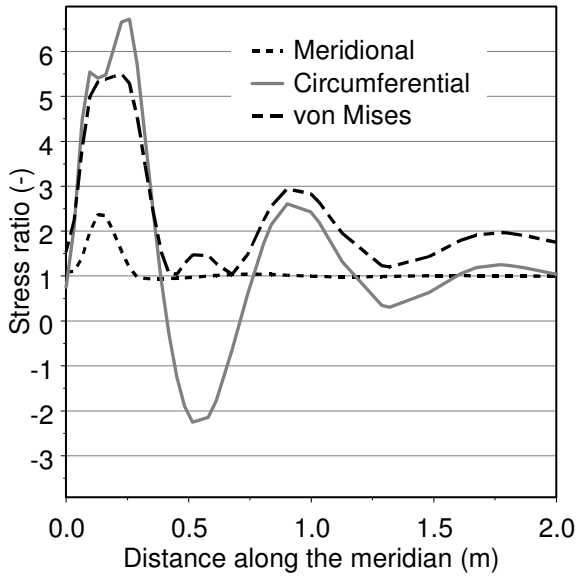


*Fig. 4.* Ratios of numerical and membrane stresses for cone 2 at maximal load

section, cone 2 is studied with other imperfection shapes. For all the shapes, the imperfection amplitude is the maximum value allowed in class C, which is for this geometry equal to 2,06 times the shell thickness. Four different imperfection shapes are investigated. Three of them are axisymmetric: the first eigenmode, an imperfection shape with one half wave in meridional direction and a weld depression. The fourth imperfection has the shape of the second eigenmode. This eigenmode has the same shape as the first eigenmode along the meridian, but exhibits one wave in circumferential direction and is therefore no longer axisymmetric. The shapes of the three axisymmetric imperfections are plotted in *Fig. 3*. The weld depression (Type A) represents a realistic deformation and was proposed by Rotter *et al.* [8].

The results of the simulations are shown in *Table 3*. For these simulations, the liquid level h' was kept constant at 6705mm. This time, the specific weight of the liquid was increased until buckling occurred. In the table, the ratio of the specific weight at failure and the specific weight of water is given. The ECCS procedure predicts for this liquid level that the ratio can reach a value of 1,62 before failure occurs. The numerical simulations lead to a different result. Where relevant, the sign of the imperfection amplitude was changed so that the orientation of the first half wave of the imperfection could be investigated. This was done for all imperfection shapes except for the weld depression since in reality this always leads to a imperfection oriented towards the central axis of the cone. The results of the GMNIA analyses show that the worst imperfection shape is the axisymmetric and outward oriented half wave, leading to a specific liquid weight at failure that is only 58% of the value predicted by the design rule. It is clear that with these imperfections, the design rule can be unconservative when yielding plays a role and will have to be modified based on a thorough study.

However, questions can be raised about the realistic nature of the imperfections. The only realistic shape that was investigated is the weld depression and this led to a specific liquid weight at failure that is larger than the predicted value by the design rule. Imperfection shapes that are (completely or partially) axisymmetric and oriented outward are very unlikely to appear in a real shell since a large amount of circumferential membrane stretching is required to obtain such a shape. Therefore, it can be considered to leave them out of the simulations. However, axisymmetric and inward oriented imperfections are fabricationally possible (as a consequence of welding) and therefore should be taken into account in the simulations.

*Table 3.* Overview of the different analysis types for the cone with geometry 2

| Type of analysis | Imperfection shape | $\gamma'_{failure} / \gamma'_{water}$ (-) | |
|---|---|---|---|
| | | Orientation of first half wave | |
| | | inward | outward |
| ECCS procedure | | 1,62 | |
| LBA | | 5,93(*) | |
| GNA | | 5,14(*) | |
| GNIA (class C) | First eigenmode | 3,13(*) | 2,73 |
| | Weld depression | 3,70(*) | - |
| MNA | | 3,63 | |
| GMNA | | 2,68 | |
| GMNIA (class C) | First eigenmode | 1,30 | 1,00 |
| | Second eigenmode | 1,09 | |
| | Axisymmetric half wave | 1,26 | 0,94 |
| | Weld depression | 1,69 | - |

(*) indicates that failure was caused by bifurcation. Other cases had snap-through buckling.

## 3 SUMMARY AND ACKNOWLEDGMENT

This contribution has shown that axisymmetric imperfection shapes in liquid-filled conical shells can lead to failure stresses that are lower than predicted by the design rule and therefore modifications of the design rule seem to be necessary. However, first an agreement has to be reached on which imperfection shapes and amplitudes should be taken into account.

The first author is a Postdoctoral Fellow of the Research Foundation – Flanders (FWO). Therefore, the authors would like to express their gratitude for the financial support of the FWO.

## REFERENCES

[1] Vandepitte, D., Rathé, J., Verhegghe, B., Paridaens, R. and Verschaeve, C., Experimental investigation of buckling of hydrostatically loaded, conical shells and practical evaluation of the buckling load, *Buckling of Shells*, pp. 375-399, Springer, Berlin, (1982).

[2] Paridaens, R., Vandepitte, D., Lagae, G., Rathé, J. and Van den Steen, A., Design equations accounting for elastic buckling of liquid-filled conical shells, *International Colloquium on Stability of Plate and Shell Structures*, April, Ghent, Proceedings, pp. 425-430, (1987).

[3] ECCS, *Buckling of Steel Shells: European Recommendations*, 4th Edition, Recommendations 8: Liquid-filled unstiffened conical shells., pp. 90-105, ECCS, Brussels, (1988).

[4] ECCS, *Buckling of Steel Shells: European Recommendations*, 5th Edition, Recommendations: Liquid-filled conical shells supported from below, under preparation.

[5] Lagae, G., Guggenberger, W., Developing the new format of the design equations for the liquid-filled conical shells, *Internal Report nr. LMO-07-10-30*, Ghent University, (2007).

[6] EN 1993-1-6, Eurocode 3:Design of steel structures-part 1-6: Strength and Stability of Shell Structures, CEN, European Committee for Standardization, Central Secretariat: rue de Stassart 36, (2007).

[7] Lagae, G., Vanlaere, W. and Van Impe, R., Plastic buckling of conical tanks with large geometrical imperfections, Jean-Pierre Jaspart, Jacques Rondal (Eds.), *Hommages á René Maquoi. (pp. 167-176),* Université de Liège, Liège, (2007).

[8] Rotter, J.M., Cylindrical shells under axial compression, J.G. Teng, J.M. Rotter (Eds.), *Buckling of Thin Metal Shells (pp. 42-87)*, Spon Press, London, (2007).